Journal of Nuclear Science and Technology

ISSN: 0022-3131 (Print) 1881-1248 (Online) Journal homepage: https://www.tandfonline.com/loi/tnst20

Thermal-Neutron Capture Cross Section and Resonance Integral of Americium-241

Shoji NAKAMURA , Masayuki OHTA , Hideo HARADA , Toshiyuki FUJII & Hajimu YAMANA

To cite this article: Shoji NAKAMURA , Masayuki OHTA , Hideo HARADA , Toshiyuki FUJII & Hajimu YAMANA (2007) Thermal-Neutron Capture Cross Section and Resonance Integral of Americium-241, Journal of Nuclear Science and Technology, 44:12, 1500-1508, DOI: 10.1080/18811248.2007.9711399

To link to this article: https://doi.org/10.1080/18811248.2007.9711399

Journal of NUCLEAR SCIENCE and TECHNOLOGY, Vol. 44, No. 12, p. 1500–1508 (2007)

ARTICLE

Thermal-Neutron Capture Cross Section and Resonance Integral of Americium-241

Shoji NAKAMURA[1,*], Masayuki OHTA[1,†], Hideo HARADA[1], Toshiyuki FUJII[2] and Hajimu YAMANA[2]

[1]*Japan Atomic Energy Agency, 2-4 Shirane, Shirakata, Tokai-mura, Naka-gun, Ibaraki-ken 319-1195*
[2]*Research Reactor Institute, Kyoto University, 2-1010 Asashiro Nishi, Kumatori-cho, Sennan-gun, Osaka 590-0494*

(Received May 28, 2007 and accepted in revised form August 31, 2007)

The thermal-neutron capture cross section ($\sigma_{0,g}$) and the resonance integral ($I_{0,g}$) leading to the ground state of ^{242}Am were measured by an activation method for neutron capture by ^{241}Am. A method with gadolinium, which was similar to the cadmium difference method, was used to measure the cross section $\sigma_{0,g}$ with attention to resonances of ^{241}Am. Americium chloride samples containing ^{241}Am radioisotope were irradiated for 68 h in the long-irradiation plug of the Kyoto University Research Reactor, KUR. Wires of Co/Al and Au/Al alloys were used as monitors to determine thermal-neutron fluxes and epithermal Westcott's indexes at the irradiation positions. An α-ray spectrometer was used to measure the activity ratios of ^{242}Cm to ^{241}Am. On the basis of Westcott's convention, the $\sigma_{0,g}$ and $I_{0,g}$ values were determined as 628 ± 22 b and 3.5 ± 0.3 kb, respectively.

KEYWORDS: americium-241, americium-242g, curium-242, activation method, thermal-neutron capture cross section, resonance integral, alpha-ray spectroscopy

I. Introduction

Associated with the social acceptability of nuclear power reactors, it would be desirable to solve the problems of the nuclear waste management of minor actinides (MAs) existing in spent nuclear fuels. The MAs (^{237}Np, ^{241}Am, ^{243}Am, *etc.*) are of importance in nuclear waste management, because the presence of these nuclides induces long-term radiotoxicity on account of their extremely long half-lives. **Figure 1** illustrates a partial section of the nuclear chart displaying relevant reactions and decays. The ^{241}Am nuclide has kept its radioactivity because of its long half-life (432.2 y[1)]), and also generates heavier actinides such as ^{242}Cm, ^{243}Cm and ^{244}Cm by further neutron captures. Since ^{242}Cm has a relatively short half-life (162.8 d[1)]), the ^{242}Cm contained in the spent nuclear fuels causes shielding and decay-heat problems. Consequently, one of the most important isotopes in MAs seems to be ^{241}Am.

A method of transmutation seems to be one of the solutions to reduce the radiotoxicity of nuclear wastes.[2)] The transmutation for several MAs makes it possible to reduce both the size of a repository for packages of nuclear wastes and the storage risks for a long term. In the study of the transmutation or burn-out of ^{241}Am by reactor neutrons, accurate data of neutron capture cross sections are necessary to evaluate the reaction rates. The accurate data with 5% error

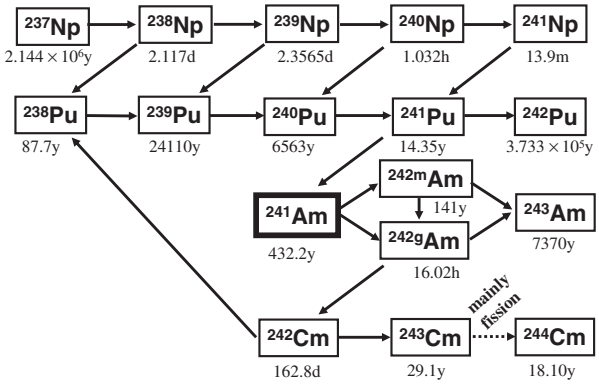

Fig. 1 Partial section of the nuclear chart displaying relevant reactions and decays

on the capture cross section of ^{241}Am have been required as registered in the World Request List for Nuclear Data: WRENDA 91/92.[3)] However, there are discrepancies among reported data for the thermal-neutron capture cross section ($\sigma_{0,g}$) and the resonance integral ($I_{0,g}$) of the ^{241}Am(n, γ)^{242g}Am reaction. Measured data[4–14)] are listed in **Table 1**. Conflicting data have been reported by many measurements for the neutron capture cross section of ^{241}Am. One finds that discrepancies between the data reported recently reach 20–30%. It seems that these discrepancies in the thermal-neutron capture cross sections may be caused by taking a cutoff energy of 0.5 eV in measurements. **Figure 2** plots the neutron cross-section curve of ^{241}Am.[15)] Since ^{241}Am has huge resonances at neutron energies of 0.308 and 0.573 eV, the cutoff energy of 0.5 eV cannot filter the first resonance.

*Corresponding author, E-mail: nakamura.shoji@jaea.go.jp
†Present address: *Osaka University, 2-1 Yamadaoka, Suita, Osaka 565-0871*

Table 1 Measured data for the ^{241}Am cross section leading to ^{242g}Am

References	Year	$\sigma_{0,g}$ (barn)	$I_{0,g}$ (barn)	Cutoff energy (eV)
Seaborg *et al.*[4)]	1946	560 ± 84		
Hanna *et al.*[5)]	1951	568 ± 56.8		
Street *et al.*[6)]	1952	300		
Pomerance[7)]	1955	625 ± 35*		
Deal *et al.*[8)]	1964	770	900	0.5
Bak *et al.*[9)]	1967	670 ± 60	2100 ± 200	0.4
Harbour *et al.*[10)]	1973	748 ± 20	1330 ± 117	0.369
Gavrilov *et al.*[11)]	1976	780 ± 50	1570 ± 10	0.5
Shinohara *et al.*[12)]	1997	768 ± 58	1694 ± 146	0.5
Fioni *et al.*[13)]	2001	636 ± 46		
Maidana *et al.*[14)]	2001	602 ± 9	1665 ± 91	0.5

The asterisk(*) denotes the cross sections of the ^{241}Am(n_{th},γ) $^{242m+g}$Am reaction.

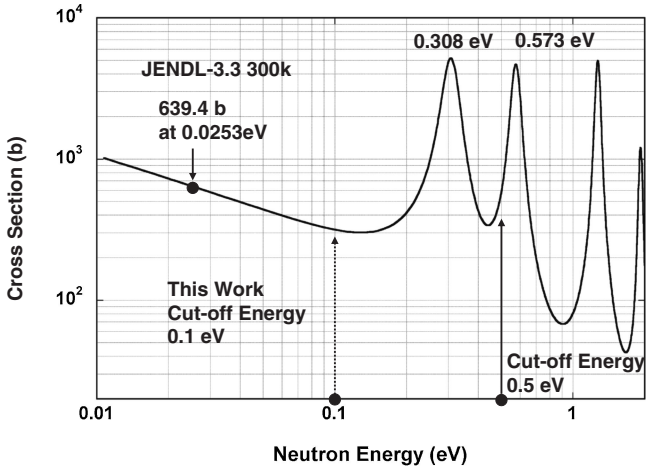

Fig. 2 The cross-section curve of ^{241}Am evaluated by JENDL-3.3.

Americium-241 has strong resonances at 0.308 and 0.573 eV, which are at least partially covering the 0.5 eV cutoff energy.

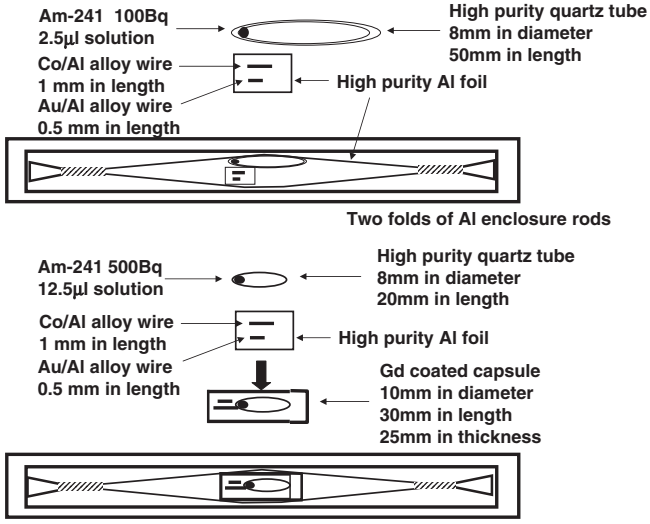

Fig. 3 Outline figures of irradiation samples

Therefore, contributions to the reaction rate by the first resonance would result in overestimation for the thermal-neutron capture cross section of ^{241}Am. In view of the behavior of the cross-section curve in Fig. 2, the cutoff energy of 0.1 eV could get rid of the influence of resonances. Thus, the aim of this work was to confirm that there would be problems in how to set the cutoff energy, and also to measure the thermal-neutron capture cross section $\sigma_{0,g}$ and the resonance integral $I_{0,g}$ of the ^{241}Am(n, γ)^{242g}Am reaction.

II. Experiments

1. Sample Preparation and Neutron Irradiation

Figure 3 schematically gives an outline of sample compositions. An ^{241}Am standardized solution (Amersham International plc., 0.5 mol/L(M) HCl) was prepared as Am samples. The Am solution contained ^{243}Am of 0.064% as one of the impurities, but its amount was very small. The energy of the α-ray from ^{243}Am is 5.3 MeV, and does not interfere with the 5.49-MeV α-ray from ^{241}Am. Even if ^{244}Cm would be generated by the neutron capture of ^{243}Am, the 5.8-MeV α-ray from ^{244}Cm also does not interfere with the 6.11-MeV α-ray from ^{242}Cm. The estimated activity of other alpha-particle emitters was negligibly 0.0002%.

Two ^{241}Am standardized solutions equivalent to 100 Bq (2.5 µl) and 500 Bq (12.5 µl) were dropped into the bottom of high-purity quartz tubes (8 mm in inner diameter, 100 mm in length) using a glass capillary without touching the inside of the tube. After drying the solutions, quartz tubes were flame-sealed under evacuation. When sealing, the bottom of the quartz tube was covered with a thick copper jacket working as a heat sink to prevent the Am sample from evaporating. The sealed tube was about 20 or 50 mm in length, and its outside was washed by 0.7 M HNO_3 and ethanol before irradiations. By measurements of the 59-keV γ ray from ^{241}Am, it was confirmed that Am samples were surely enclosed in quartz tubes.

Wires of Co/Al alloy (Co: 0.46 ± 0.1 wt%, 0.381 mm in diameter) and Au/Al alloy (Au: 0.112 ± 0.01 wt%, 0.510 mm in diameter) were used to monitor neutron fluxes at the irradiation position. Since ^{59}Co and ^{197}Au have different sensitivities to thermal and epithermal neutrons, those wires are appropriate for determining the thermal and epithermal

Table 2 Nuclear data used for the neutron-flux monitors[1,18,19]

Material	Amounts[a] (mg)	Irradiation time	Irradiation type	Half-life[a]	σ_0[a] (barn)	I_0[a] (barn)	g	s_0[a]	G_{th}	G_{epi}	Detected γ-rays Energy (keV)	Detected γ-rays $I\gamma$[b] (%)
Co/Al alloy Co:0.46 wt% 0.381 mmϕ	#1 0.3863 $_2$	10 h	without the Gd	5.2714 $_5$	37.18 $_6$	75.9 $_{20}$	1.0004	1.738 $_{61}$	1.00	1.00	1173	99.9736 $_7$
	#2 0.5991 $_2$	10 h	with the Gd	y							1332	99.9856 $_4$
Au/Al alloy Au:0.112 wt% 0.510 mmϕ	#1 0.3346 $_2$	10 h	without the Gd	2.69517 $_{21}$	98.65 $_9$	1550 $_{28}$	1.0054	17.22 $_{32}$	1.00	0.99	412	95.58 $_{12}$
	#2 0.6599 $_2$	10 h	with the Gd	d								

[a] In our notation, 0.3863 $_2$ is 0.3863 $\pm$ 0.0002, 5.2714 $_5$ is 5.2714 $\pm$ 0.0005, 75.9 $_{20}$ is 75.9 $\pm$ 2.0, *etc.*
[b] Gamma-ray emission probability per decay. In our notation, 99.9736 $_7$ is 99.9736 $\pm$ 0.0007, *etc.*

fractions in the neutron flux.[16,17] The amount of Co or Au contained in each wire was determined by weight measurement with a microbalance. Nuclear data[1,18,19] for monitor wires are listed in **Table 2**. A set of Co and Au monitor wires were wrapped with a high-purity aluminum foil, and attached to the sealed tube. When samples were housed in two-fold–aluminum-enclosure rods, samples were wrapped with aluminum foils in the shape of a string as shown in Fig. 3 so as not to slip off from irradiation positions. The enclosure rod was sealed by electric welding.

In this work, attention was paid to huge resonances of ^{241}Am at 0.573 and 0.308 eV as shown in Fig. 2. If the cutoff energy is set as 0.1 eV, it could avoid those resonances. Hence, a gadolinium (Gd) foil was used as a filter. Since Gd has a large capture cross section of 10000 b, it would be effective for filtering thermal neutrons. An aluminum capsule, 10 mm in diameter and 30 mm in length, was prepared to put the Am-sealed tube in it. A Gd foil was coated on the outside surface of the aluminum capsule. The thickness of the Gd foil was optimized in the neutron transmission. Results of transmission in changing the thickness of Gd foils are plotted in **Fig. 4**. When the Gd foil with a 25 µm thickness is used, the effective thickness is estimated as 35 µm in consideration of the geometric shape of the capsule. The energy at which transmission is reduced by half can be estimated as 0.107 eV as seen from Fig. 4. Hence, the Gd foil with a 25 µm thickness was chosen, and the cutoff energy was set as 0.107 eV in this experiment. As shown at the bottom of Fig. 3, the Am sample and monitors were housed in the Gd-coated capsule, and the capsule was further loaded into another aluminum enclosure rod.

The irradiations with and without the Gd-coated capsule were performed for 68 h in the long-irradiation (LI) plug of the KUR, of which the nominal value of the thermal-neutron flux was 4.7×10^{13} n/cm^{2}s when operating at 5 MW. The rod loading Gd-shielded samples was arranged at a lower position in the LI plug, and the other rod was arranged at an upper position. Thus, the samples with and without the Gd-coated capsule were kept away at about 40 cm in the vertical direction so as not to interfere with each other. For irradiations, it is important to avoid the population of ^{242}Cm caused by ^{242m}Am, *i.e.*, there is an optimal irradiation time. Under the present conditions, the induced activity of ^{242m}Am and its contribution to ^{242}Cm were negligible both because

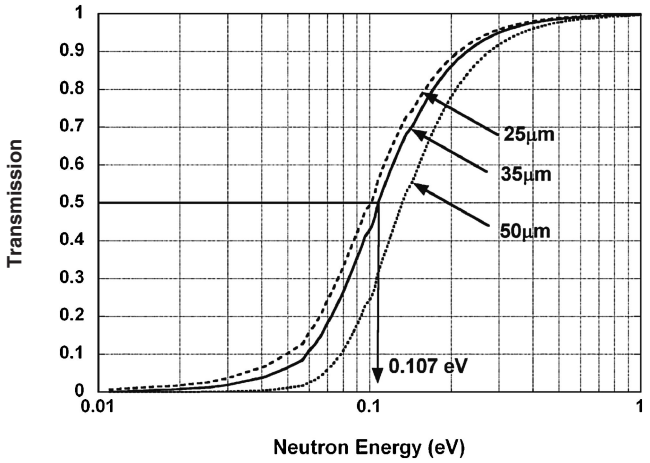

Fig. 4 Transmission of neutrons through the Gd foils with various thicknesses.
The solid line plots the transmission through the Gd foil with a 35 µm thickness, the broken line a 25 µm thickness, and the dotted line a 50 µm thickness.

^{241}Am has a small cross section to produce ^{242m}Am in comparison with that of ^{242g}Am and because ^{242m}Am has a relatively long half-life of 141 y.[1] Thus, ^{242}Cm was accumulated only via the ^{241}Am(n, γ)^{242g}Am reaction. After allowing ^{242g}Am (16.02 h[1]) to decay for 18 d, the α-ray activity of ^{242}Cm was measured relative to the ^{241}Am sample activity as described in the next section.

2. Activity Measurement

Two irradiated Am samples with and without the Gd-coated capsule were dissolved by adding 30 µl of 3 M HNO_3 solution. About 10 µl was extracted from each solvent solution, and was dropped onto the center of a Petori laboratory dish (30 mmϕ in diameter, 10 mm in height). After dryness, measurement samples were prepared. To check the reproducibility of measurements, three measurement samples were made from each irradiated Am sample. Alpha rays emitted from ^{241}Am (5.5 MeV) and ^{242}Cm (6.1 MeV) were measured with a silicon surface-barrier alpha-spectrometer (SEIKO EG&G ORTEC SOLOIST Alpha Spectrometer). Measurements were performed for 1–2 h until more than 10 k counts were obtained for a peak area originating from ^{242}Cm.

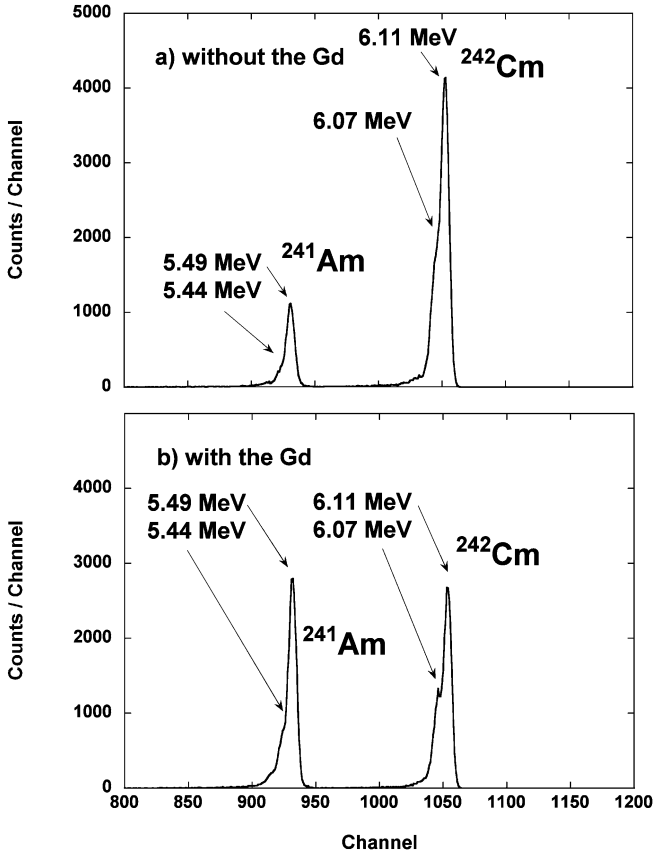

Fig. 5 Examples of α-ray spectra of irradiated Am samples. a) The upper side shows the spectrum of the bare ^{241}Am sample; b) the lower side shows the spectrum of the ^{241}Am sample irradiated with the Gd-coated capsule.

Figure 5 shows typical α-ray spectra obtained from the Am samples in the irradiations with and without the Gd-coated capsule. The measured system resolution for the α-ray peaks of ^{241}Am and ^{242}Cm was 45 keV.

The γ rays from irradiated monitor wires were measured by a high-purity Ge detector, the performance of which was characterized by a relative efficiency of 25% to a 7.6 cm $\times$ 7.6 cmϕ NaI (Tl) detector and an energy resolution of 1.9 keV full width at half-maximum (FWHM) at the 1.33 MeV peak of ^{60}Co. The peak detection efficiencies were determined with a set of calibrated mixed sources: ^{113}Sn, ^{137}Cs, ^{88}Y and ^{60}Co. The error of the detection efficiency due to the uncertainties of the calibration γ source intensities was estimated as 2%. The radioactivities of Au and Co monitor wires were measured at a distance of 200 mm from the center of the detector head.

III. Analysis

1. Outline of Westcott's Convention

The effective cross section $\hat{\sigma}$ is defined by equating the reaction rate R to the product of $\hat{\sigma}$ and $n\upsilon_0$, where $n\upsilon_0$[16,17] is the "neutron flux" in Westcott's convention[20] with the neutron density n, including thermal and epithermal neutrons, and with the velocity of neutrons $\upsilon_0 = 2{,}200$ m/s, so that

$$R = n\upsilon_0\hat{\sigma}. \tag{1}$$

When the cross section departs from the $1/\upsilon$ law, a simple relation for $\hat{\sigma}$ can be obtained as:

$$\hat{\sigma} = \sigma_0(gG_{th} + r(T/T_0)^{1/2}s_0G_{epi}), \tag{2}$$

where σ_0 is the thermal-neutron capture cross section; g is a function of the temperature related to the departure of the cross section from the $1/\upsilon$ law; r is an epithermal index in Westcott's convention; T is the neutron temperature and T_0 is 293.6 K; the quantity $r(T/T_0)^{1/2}$ gives the fraction of epithermal neutrons in the neutron spectrum; the G_{th} and G_{epi} denote self-shielding coefficients for thermal and epithermal neutrons, and are taken as unity in this analysis under the present sample conditions. The value of g for ^{241}Am was taken as 1.051.[18] The parameter s_0 is defined as:

$$s_0 = \frac{2I_0'}{\sqrt{\pi}\sigma_0}, \tag{3}$$

where I_0' is the reduced resonance integral, *i.e.*, the resonance integral with the $1/\upsilon$ component subtracted.

2. Flux and Cross-Section Determination with Simplified Equations

Substituting Eq. (3) into Eq. (1), reaction rates can be written in simplified forms as:

$$R/\sigma_0 = gG_{th}\phi_1 + G_{epi}\phi_2 s_0, \tag{4}$$

for irradiation without the Gd-coated capsule, and

$$R'/\sigma_0 = gG_{th}\phi_1' + G_{epi}\phi_2' s_0, \tag{5}$$

for irradiation with the Gd-coated capsule. Here, the ϕ_1 and ϕ_1' are neutron fluxes in the low (thermal) energy region. The ϕ_2 and ϕ_2' are those in the epithermal energy region. The prime ($'$) refers to irradiation with the Gd-coated capsule. The values of ϕ_1, ϕ_2, ϕ_1' and ϕ_2' at the irradiation position were obtained by using s_0 and σ_0 in Table 2 and reaction rates R and R' for the monitor wires. The reaction rates were calculated from peak counts of γ rays from ^{60}Co and ^{198}Au. **Figure 6** shows the experimental relation between R/σ_0 (or R'/σ_0) and s_0 obtained by the flux monitor wires. The neutron fluxes ϕ_1 and ϕ_1' are obtained with the relation in Fig. 6; the slope of each solid line gives the epithermal flux, *i.e.*, ϕ_2 or ϕ_2'. The irradiation positions of two targets were kept away at about 40 cm from the core center in the vertical direction at the KUR so as not to interfere with each other. The results of the neutron fluxes are tabulated in **Table 3**. The thermal-neutron flux at the irradiation position was $(3.03 \pm 0.11) \times 10^{13}$ n/cm^2/s, and its error was mainly based on the errors of the detection efficiency and the cross sections used in this analysis.

From Eqs. (4) and (5), the parameter s_0 is rewritten as follows:

$$s_0 = -\frac{gG_{th}\phi_1 - gG_{th}\phi_1'(R/R')}{\phi_2 G_{epi} - \phi_2' G_{epi}(R/R')}, \tag{6}$$

and s_0 is obtained from the ratio of R to R' for irradiated targets and the neutron fluxes ϕ_1, ϕ_2, ϕ_1' and ϕ_2', which are

Table 3 Reaction rates for monitors and neutron flux in long-irradiation plug at KUR

$\times 10^{13}$ (n/cm^2·s)

	R/σ_0 (without the Gd)	R'/σ_0 (with the Gd)	Thermal neutron flux ϕ_1 or ϕ_1'	Epithermal neutron flux ϕ_2 or ϕ_2'
^{60}Co	3.19 ± 0.10	0.515 ± 0.016	$\phi_1 = 3.03 \pm 0.11$	$\phi_2 = 0.090 \pm 0.009$
^{198}Au	4.58 ± 0.10	2.18 ± 0.05	$\phi_1' = 0.391 \pm 0.019$	$\phi_2' = 0.108 \pm 0.004$

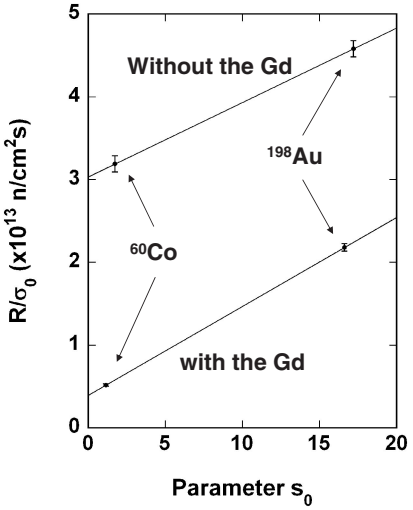

Fig. 6 Experimental relations between R/σ_0 and s_0 obtained by analysis of the induced activities of flux monitors

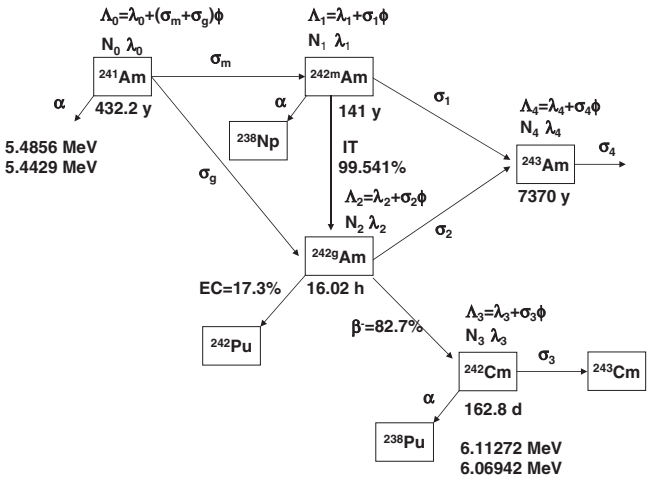

(a)

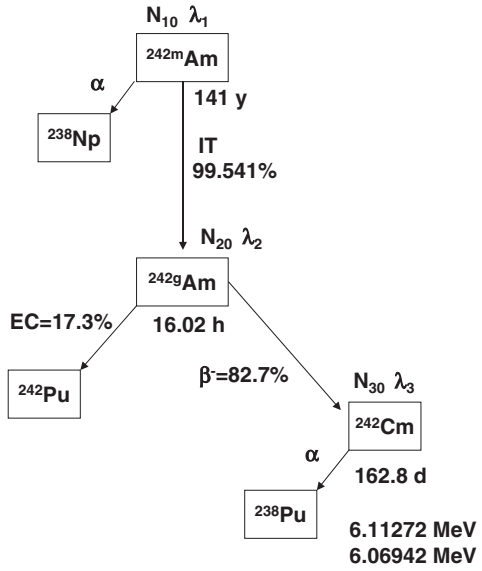

(b)

Fig. 7 (a) Neutron capture and decay process of ^{241}Am and products in neutron irradiation (b) Decay scheme of product nuclei after irradiation

tabulated in Table 3. The σ_0 is obtained by substituting s_0 into Eq. (4). The I_0' is then obtained using Eq. (3).

The resonance integral I_0 is expressed by the following equation:

$$I_0 = I(1/\upsilon) + I_0', \tag{7}$$

where the term $I(1/\upsilon)$ in Eq. (7) is the $1/\upsilon$ contribution to the resonance integral above the cutoff energy (E_c) and derived as:

$$I(1/\upsilon) = \int_{E_C}^{\infty} g\sigma_0 \sqrt{\frac{E_0}{E}} \frac{dE}{E} = 2g\sigma_0 \sqrt{\frac{E_0}{E_C}}, \tag{8}$$

where E_0 is the thermal neutron energy (0.0253 eV). For $E_c = 0.107$ eV, the $1/\upsilon$ contribution to the resonance integral is estimated to be $I(1/\upsilon) = 1.022\sigma_0$ from Eq. (8). Then, the resonance integral I_0 is given as:

$$I_0 = I_0' + 1.022\sigma_0. \tag{9}$$

3. Analysis of Reaction Rate for ^{241}Am(n_{th},γ)^{242g}Am Reaction

Figure 7(a) shows the neutron capture reactions and decay chains related to ^{241}Am during neutron irradiation. The symbols in Fig. 7(a) denote the following: the subscripts 0, 1, 2, 3 and 4 denote ^{241}Am, ^{242m}Am, ^{242g}Am, ^{242}Cm and ^{243}Am nuclei, respectively; N is the number of nuclei; λ is the decay constant; σ_m and σ_g are the neutron capture cross sections leading to ^{242m}Am and ^{242g}Am, respectively; σ_1, σ_2, σ_3 and σ_4 are the capture σ_γ and fission cross sections σ_f for ^{242m}Am, ^{242g}Am, ^{242}Cm and ^{243}Am, respectively. Nuclear data used in this analysis are listed in **Table 4**.

The amount N_1 of ^{242m}Am is given by

$$N_1 = \frac{N_0\sigma_m\phi}{\Lambda_1 - \Lambda_0}(\exp(-\Lambda_0 t_{irr}) - \exp(-\Lambda_1 t_{irr})), \tag{10}$$

$$\Lambda_0 \equiv \lambda_0 + (\sigma_m + \sigma_g)\phi, \text{ and } \Lambda_1 \equiv \lambda_1 + \sigma_1\phi,$$

Table 4 Nuclear data used for the cross-section determination[1,18,19)]

Nuclide	Half-life	Decay (branch:%)		Cross sections (b) Capture σ_γ, fission σ_f	Resonance integral (b) Capture I_γ, fission I_f
^{241}Am	432.2 ± 0.7 y	α (100)	5486 keV (84.5)	$\sigma_\gamma = 54 \pm 5$ (to 242 m)	$I_\gamma = 195 \pm 20$ (to 242 m)
			5443 keV (13.0)	$\sigma_\gamma = 533 \pm 13$ (to 242 g)	$I_\gamma = 1230 \pm 100$ (to 242 g)
			…, *etc.*	$\sigma_f = 3.20 \pm 0.09$	$I_f = 14.4 \pm 1.0$
^{242m}Am	141 ± 2 y	IT: 99.541 ± 0.012		$\sigma_\gamma = 2000 \pm 600$	
				$\sigma_f = 6950 \pm 280$	$I_f = 1800 \pm 65$
^{242g}Am	16.02 ± 0.02 h	β^-: 82.7 ± 0.3		$\sigma_\gamma = 2100 \pm 200$	—
^{242}Cm	162.8 ± 0.2 d	α (100)	6113 keV (74.0)	$\sigma_\gamma = 16 \pm 5$	$I_\gamma = 110 \pm 20$
			6069 keV (25.0)	$\sigma_f < 5$	
			…, *etc.*		
^{243}Am	7370 ± 40 y	α (100)	5275 keV (87.4)	$\sigma_\gamma = 75.1 \pm 1.8$	$I_\gamma = 1820 \pm 70$
			5233 keV (11.0)		
			…, *etc.*		
^{238}Pu	87.7 ± 0.3 y	α (100)	5499 keV (70.91)		
			5456 keV (28.98)		
			…, *etc.*		

where ϕ is the neutron flux; t_{irr} is the neutron irradiation time.

In consideration of the loss of ^{241}Am sample amount during irradiation, the amount N_2 of ^{242g}Am can be written in the form:

$$\frac{dN_2}{dt} = N_0\sigma_g\phi + IT \cdot \lambda_1 N_1 - \lambda_2 N_2 - N_2\sigma_2\phi \approx N_0\sigma_g\phi - \Lambda_2 N_2 = N_0\sigma_g\phi \cdot \exp(-\Lambda_0 t) - \Lambda_2 N_2, \quad (11)$$

$$\Lambda_2 \equiv \lambda_2 + \sigma_2\phi,$$

where IT is the isomer transition probability (99.541%[1)]) from ^{242m}Am to ^{242g}Am. Although 100 Bq of the ^{241}Am sample would be irradiated for a week, the induced activity of ^{242m}Am could be estimated as only 0.3 Bq because of its long half-life (141 y[1)]). Thus, the contribution of the isomer transition from ^{242m}Am to ^{242g}Am is negligible under the present irradiation conditions.

One can derive its solution:

$$N_2(t) = \frac{N_0\sigma_g\phi}{\Lambda_2 - \Lambda_0}(\exp(-\Lambda_0 t) - \exp(-\Lambda_2 t)). \quad (12)$$

Consequently, the amount N_3 of ^{242}Cm is given by

$$\frac{dN_3}{dt} = \beta \cdot \lambda_2 N_2 - \lambda_3 N_3 - N_3\sigma_3\phi = \beta \cdot \lambda_2 N_2 - \Lambda_3 N_3, \quad (13)$$

$$\Lambda_3 \equiv \lambda_3 + \sigma_3\phi,$$

where β is the branching ratio (82.7 ± 0.3%[1)]) of ^{242g}Am decaying to ^{242}Cm. Then, the following solution can be obtained:

$$N_3(t) = \frac{\beta \cdot \lambda_2 N_0\sigma_g\phi}{(\Lambda_2 - \Lambda_0)(\Lambda_3 - \Lambda_0)} \times (\exp(-\Lambda_0 t) - \exp(-\Lambda_3 t)) + \frac{\beta \cdot \lambda_2 N_0\sigma_g\phi}{(\Lambda_2 - \Lambda_0)(\Lambda_3 - \Lambda_2)} \times (\exp(-\Lambda_3 t) - \exp(-\Lambda_2 t)). \quad (14)$$

The decay scheme of products after irradiation is illustrated in Fig. 7(b). When the time of the end of irradiation is taken on the standard of time, changes for the number of nuclei in the decay of ^{242g}Am after irradiation can be given by the following equation:

$$N_2^*(t) = N_{20} \cdot \exp(-\lambda_2 t), \quad (15)$$

where N_{20} is the number of nuclei of ^{242g}Am at the end time of irradiation, and is given by replacing t with t_{irr} in Eq. (12):

$$N_{20} \equiv \frac{N_0\sigma_g\phi}{\Lambda_2 - \Lambda_0}(\exp(-\Lambda_0 t_{irr}) - \exp(-\Lambda_2 t_{irr})). \quad (16)$$

Similarly, the population from ^{242g}Am to ^{242}Cm is described by the following equation:

$$\frac{dN_3^*}{dt} = \beta \cdot \lambda_2 N_{20} \exp(-\lambda_2 t) - \lambda_3 N_3. \quad (17)$$

Then, the solution is derived as follows:

$$N_3^*(t) = \frac{\beta \cdot \lambda_2 N_{20}}{\lambda_3 - \lambda_2} \cdot (\exp(-\lambda_2 t) - \exp(-\lambda_3 t)) + N_{30} \cdot \exp(-\lambda_3 t), \quad (18)$$

where N_{30} is the number of nuclei of ^{242}Cm at the end of irradiation, and given by replacing t with t_{irr} in Eq. (14), *i.e.*,

$$N_{30} = \frac{\beta \cdot \lambda_2 N_0\sigma_g\phi}{(\Lambda_2 - \Lambda_0)(\Lambda_3 - \Lambda_0)} \times (\exp(-\Lambda_0 t_{irr}) - \exp(-\Lambda_3 t_{irr})) + \frac{\beta \cdot \lambda_2 N_0\sigma_g\phi}{(\Lambda_2 - \Lambda_0)(\Lambda_3 - \Lambda_2)} \times (\exp(-\Lambda_3 t_{irr}) - \exp(-\Lambda_2 t_{irr})). \quad (19)$$

If the cooling time t_c is replaced with the time from the end of irradiation to the start of the measurement, the radioactivity A_3 at the beginning of the measurement can be given by the following equation:

Table 5 Experimental results of the Cm/Am yield ratio and the reaction rates

without the Gd	Cm/Am yield ratio	Reaction rate R_g ($\times 10^{-8}$/s)	with the Gd	Cm/Am ratio	Reaction rate R'_g ($\times 10^{-9}$/s)
#1	4.144 ± 0.059	2.307 ± 0.035	#1	1.071 ± 0.013	5.926 ± 0.075
#2	4.106 ± 0.056	2.282 ± 0.033	#2	1.089 ± 0.012	6.027 ± 0.069
#3	4.138 ± 0.043	2.293 ± 0.026	#3	1.078 ± 0.009	5.968 ± 0.056
	w.a.	**2.293 ± 0.019**		**w.a.**	**5.975 ± 0.043**

Table 6 Systematic errors due to the nuclear data used in this analysis

Nuclide	Item	Error (%)	Nuclide	Item	Error (%)
^{241}Am	Half-life: $T_{1/2}$	0.16	^{244}Cm	Half-life: $T_{1/2}$	0.1
	Cross section: σ_r,σ_f	0.13		Cross section: σ_r,σ_f	*negligibly small*
^{242m}Am	Half-life: $T_{1/2}$	*negligibly small*	—	Branching ratio β^-	0.36
	Cross section: σ_r,σ_f				
^{242g}Am	Half-life: $T_{1/2}$	*negligibly small*	—	Isomer transition probability: *IT*	*negligibly small*
	Cross section: σ_r	0.05			
^{243}Am	Half-life: $T_{1/2}$	*negligibly small*	—	Irradiation time: t_{irr}	0.12
	Cross section: σ_r			Cooling time: t_c	0.003

Total systematic error: 0.45(%)

$$\begin{aligned} A_3 &= \lambda_3 N_3^*(t_c), \\ &= \frac{\beta \cdot \lambda_2\lambda_3 N_{20}}{\lambda_3 - \lambda_2} \cdot (\exp(-\lambda_2 t_c) - \exp(-\lambda_3 t_c)) \\ &\quad + \lambda_3 N_{30} \cdot \exp(-\lambda_3 t_c). \end{aligned} \tag{20}$$

When the α-ray yields originating from ^{241}Am and ^{242}Cm are expressed with Y_0 and Y_3, respectively, the ^{242}Cm/^{241}Am activity ratio can be given by

$$\begin{aligned} \frac{Y_3}{Y_0} &= \frac{\beta \cdot \lambda_2\lambda_3 N_{20}(\exp(-\lambda_2 t_c) - \exp(-\lambda_3 t_c))}{(\lambda_3 - \lambda_2)\lambda_0 N_0 \cdot \exp(-\Lambda_0 t_{irr})} \\ &\quad + \frac{\lambda_3 N_{30} \cdot \exp(-\lambda_3 t_c)}{\lambda_0 N_0 \cdot \exp(-\Lambda_0 t_{irr})}. \end{aligned} \tag{21}$$

There is an advantage that the measuring time, dead time corrections, absolute efficiencies and a correction for a solid angle are all canceled due to the relative measurement. Substituting Eqs. (16) and (19) into Eq. (21), it is arranged with the reaction rate $R_g \equiv \sigma_g \phi$. One can obtain the following equation:

$$\begin{aligned} \frac{Y_3}{Y_0} &= R_g \cdot \frac{\beta \cdot \lambda_2\lambda_3}{\lambda_0(\lambda_3 - \lambda_2)(\Lambda_2 - \Lambda_0) \cdot \exp(-\Lambda_0 t_{irr})} \\ &\quad \times (\exp(-\Lambda_0 t_{irr}) - \exp(-\Lambda_2 t_{irr})) \\ &\quad \times (\exp(-\lambda_2 t_c) - \exp(-\lambda_3 t_c)) \\ &\quad + R_g \cdot \frac{\beta \cdot \lambda_2\lambda_3}{\lambda_0(\Lambda_2 - \Lambda_0)(\Lambda_3 - \Lambda_0) \cdot \exp(-\Lambda_0 t_{irr})} \\ &\quad \times (\exp(-\Lambda_0 t_{irr}) - \exp(-\Lambda_3 t_{irr})) \cdot \exp(-\lambda_3 t_c) \\ &\quad + R_g \cdot \frac{\beta \cdot \lambda_2\lambda_3}{\lambda_0(\Lambda_2 - \Lambda_0)(\Lambda_3 - \Lambda_2) \cdot \exp(-\Lambda_0 t_{irr})} \\ &\quad \times (\exp(-\Lambda_3 t_{irr}) - \exp(-\Lambda_2 t_{irr})) \cdot \exp(-\lambda_3 t_c). \end{aligned} \tag{22}$$

Thus, the reaction rate R_g can be calculated from the α-activity ratio with Eq. (22).

IV. Results and Discussion

From the α-activity ratios of 162-d ^{242}Cm to 432-y ^{241}Am, as determined by the silicon surface barrier alpha spectrometer, the reaction rates R_g were obtained as listed in **Table 5**. The statistical error in the α-ray measurements was about 1%. The systematic errors resulting from the nuclear data used in this analysis were examined quantitatively as listed in **Table 6**. The total systematic error was found to be very small as 0.45% because of the following reasons: (1) the detection efficiency in the α-ray measurements was canceled; (2) the accuracy of the half-life data used in this analysis was very high; (3) the influences of the multiple neutron capture and fission reactions were negligible.

Solving Eqs. (4) and (5) with the information on the obtained reaction rates R_g and the neutron fluxes, one finds the thermal-neutron capture cross section $\sigma_{0,g}$ and the parameter s_0. Furthermore, the resonance integral $I_{0,g}$ was calculated with the parameter s_0 from Eqs. (3) and (9). For the ^{241}Am$(n,\gamma)^{242g}$Am reaction, the thermal-neutron capture cross section $\sigma_{0,g}$ was obtained as 628 ± 22 b. The resonance integral $I_{0,g}$ was obtained as 3.5 ± 0.3 kb when the cutoff energy was 0.107 eV. The errors of the thermal-neutron capture cross section $\sigma_{0,g}$ and the resonance integral $I_{0,g}$ were estimated by the error propagation due to the errors of the reaction rates R_g and the neutron fluxes. The present results are summarized in **Table 7** together with the evaluated values.[15,18,21,22] The present results are the cross sections for the formation of the ground state of ^{242}Am. On the other hand, the evaluated values include the cross sections for the formation of the isomer and ground states of ^{242}Am. Therefore, the present results cannot be simply compared with the evaluated values.[15,21,22] When the cross section producing the isomer state of ^{242}Am is taken into account with the branching ratio (0.90 ± 0.09) obtained by Shinohara *et*

Table 7 Present results and the evaluated data

References	$\sigma_{0,g}$ (barn)	$I_{0,g}$ (barn)	Cutoff energy (eV)	Parameter s_0
Present work	**628 ± 22**	**3.5 ± 0.3 k**	**0.107**	**5.21 ± 0.51**
JENDL-3.3[15]	639.4*	1456*		
Maghabghab[18]	533 ± 13	1230 ± 100	0.5	
JEFF3.1[21]	647.04*	1526.4*		
ENDF-VII.0[22]	620.84*	—		

An asterisk(*) denotes the cross sections of the ^{241}Am(n,γ) $^{242m+g}$Am reaction.

al.,[12] the capture cross section $\sigma_{0,m+g}$ would be roughly estimated as about 690 b from the present result, and about 8% larger than the JENDL-3.3 evaluation (639.47 b[15]). The evaluation is probably done for the ^{241}Am cross section under the limitation of the total cross-section data (654.4 b). It seems that total cross section itself is underestimated in view of the present result.

As shown in Table 1, Hanna *et al.*[5] measured a cross section for pile neutrons, and obtained 568 ± 56.8 b for ^{241}Am leading to the production of ^{242}Cm. Street *et al.*[6] reported a pile neutron capture cross section of 300 b for the ^{241}Am$(n,\gamma)^{242g}$Am reaction, which was derived from an observed cross section of 200 b for the formation of ^{242}Cm and 60% β^- branching of ^{242m}Am. Pomerance measured the thermal-neutron capture cross section of 625 ± 35 b based on the value of 98 b for gold in the reactor oscillator.[7] It should be noted that these neutron capture cross sections are for a pile neutron spectrum. Thus, these cross sections could conceivably vary with different reactors and irradiation positions.

The possible reason for the disagreement on the thermal-neutron capture cross section among the data would be found in the fact that the ^{241}Am has two very strong resonances at 0.308 and 0.573 eV, which are at least partially covering the cutoff energy. The presence of these resonances affects the sample activities, and should be taken into account. Fioni *et al.*[13] measured the capture cross section of ^{241}Am at the high-flux reactor of the Institute Laue-Langevin in Grenoble. They used the H9 irradiation tube providing thermal neutrons (only 2% of epithermal neutrons) so that their measurement was not necessary to consider the effects of the resonances of ^{241}Am. Maidana *et al.*[14] measured the thermal-neutron cross section and resonance integral for the ^{241}Am$(n,\gamma)^{242g}$Am reaction by the activation method at the IPEN 2 MW pool-type research reactor. They considered the effects from the resonances for sample activities by means of a Monte Carlo simulation. The reason why the results by Fioni and Maidana *et al.* are close to the present result may be due to their data treatments.

Figure 8 shows the dependence of the ^{241}Am resonance integral on the cutoff energy. The solid line plots the resonance integral as a function of the cutoff energy from the data of JENDL-3.3, which includes the contribution of ^{242g}Am. It is difficult to interpret the differences between reported values of $I_{0,g}$ shown in Fig. 8. Since Gavrilov *et al.*[11] and Shinohara *et al.*[12] measured the resonance integrals at a 0.5 eV cutoff energy with a 1-mm-thick cadmium shield, it

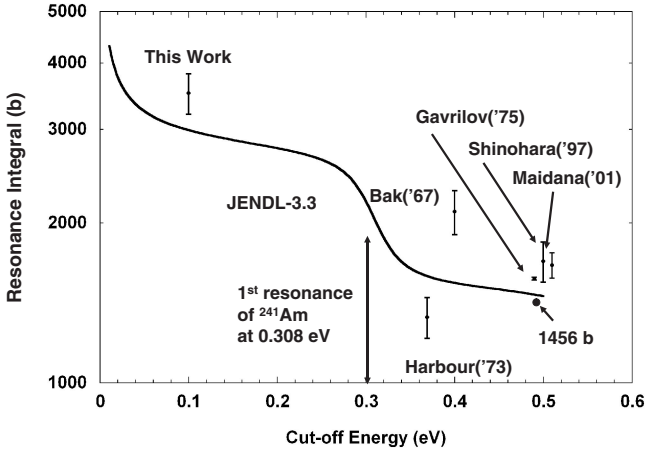

Fig. 8 Dependences on cutoff energies for the resonance integral of ^{241}Am

seems that there is no problem with their results. One can conclude that the evaluation would be underestimated for the resonance integral $I_{0,g}$.

V. Conclusion

The thermal-neutron capture cross section and the resonance integral of the ^{241}Am$(n,\gamma)^{242g}$Am reaction were measured by the activation method. With careful attention to the first resonance of ^{241}Am, the cutoff energy was taken as 0.107 eV with the Gd-coated capsule having appropriate thickness. The thermal-neutron capture cross section $\sigma_{0,g}$ was obtained as 628 ± 22 b on the basis of Westcott's convention. The present result became smaller than that obtained by previous measurements, because the influences of the resonances of ^{241}Am were eliminated with the Gd-coated capsule. Thus, we conclude that part of the previous measurements gave an overestimation to the thermal-neutron capture cross section. The resonance integral $I_{0,g}$ was obtained as 3.5 ± 0.3 kb. As a matter of course, it became much larger than the past data because of the 0.107 eV cutoff energy.

Acknowledgments

The authors would like to appreciate H. Kodaka, K. Miyata and J. Takada of the Research Reactor Institute of Kyoto University for their cooperation. One of the authors

(S.N.) is grateful to K. Furutaka for valuable information and suggestions.

This work has been carried out in part under the Visiting Researcher's Program of the Research Reactor Institute, Kyoto University.

References

1) R. B. Firestone, V. S. Shirley, C. M. Baglin, S. Y. F. Chu, J. Zipkin, *Table of Isotopes*, 8th edition, John Wiley & Sons, New York, (1995).
2) H. Takano, T. Ikegami, "Actinides on R&D of partitioning and transmutation in Japan," *Actinide and Fission Product Partitioning and Transmutation, Seventh Information Exchange Meeting*, Jeju, Republic of Korea, Oct. 14–16, 2002, 23–35, (2002).
3) N. Kocherov, P. K. McLaughlin (Eds.), *World Request List for Nuclear Data*, INDC(SEC)-104 (1993).
4) G. T. Seaborg, W. M. Manning, *Capture Cross Section of Americium-241 for Pile Neutrons*, Chicago University Metallurgical Labs Reports, No. 3471, 4 (1946).
5) G. C. Hanna, B. G. Harvey, N. Moss, "The neutron capture cross section of Am^{241}," *Phys. Rev.*, **81**, 486 (1951).
6) K. Street, Jr., A. Ghiorso, S. G. Thompson, "Slow neutron fission of Am^{242}, Am^{242m}, and Am^{243*}," *Phys. Rev.*, **85**, 135 (1952).
7) H. Pomerance, ORNL-1879, 50 (1955).
8) R. A. Deal, R. P. Schuman, WASH-1053, 76 (1964).
9) M. A. Bak, A. S. Krivokhatskii, K. A. Petrzhak, Yu. G. Petrov, Yu. F. Romanov, E. A. Shlyamin, "Cross sections and resonance integrals for capture and fission in long-lived americium isotopes," *Sov. At. Energy*, **23**, 1059 (1967).
10) R. M. Harbour, K. W. MacMurdo, F. J. McCrosson, "Thermal-neutron capture cross sections and capture resonance integrals of americium-241," *Nucl. Sci. Eng.*, **50**, 364 (1973).
11) V. D. Gavrilov, V. A. Goncharov, V. P. Smirnov, "Thermal cross sections and resonance integrals of fission and capture of ^{241}Am, ^{243}Am, ^{245}Cm, ^{249}Bk, and ^{249}Cf," *Sov. At. Energy*, **41**[3], 808 (1976).
12) N. Shinohara, Y. Hatsukawa, K. Hata, N. Kohno, "Radiochemical determination of neutron capture cross sections of ^{241}Am," *J. Nucl. Sci. Technol.*, **34**[7], 613 (1997).
13) G. Fioni, M. Cribier, F. Marie *et al.*, "Incineration of 241Am induced by thermal neutrons," *Nucl. Phys. A*, **693**, 546 (2001).
14) N. L. Maidana, M. S. Dias, M. F. Koskinas, "Measurement of the thermal neutron capture cross section and resonance integral of Am-241," *Radiochim. Acta.*, **89**, 419 (2001).
15) K. Shibata, T. Kawano, T. Nakagawa, O. Iwamoto, J. Katakura, T. Fukahori, S. Chiba, A. Hasegawa, T. Murata, H. Matsunobu, T. Ohsawa, Y. Nakajima, T. Yoshida, A. Zukeran, M. Kawai, M. Baba, M. Ishikawa, T. Asami, T. Watanabe, Y. Watanabe, M. Igashira, N. Yamamuro, H. Kitazawa, N. Yamano, H. Takano, "Japanese evaluated nuclear data library version 3 revision-3: JENDL-3.3," *J. Nucl. Sci. Technol.*, **39**, 1125 (2002).
16) T. Katoh, S. Nakamura, K. Furutaka, H. Harada, K. Fujiwara, T. Fujii, H. Yamana, "Measurement of thermal neutron capture cross section and resonance integral of the ^{237}Np$(n,\gamma)^{238}$Np reaction," *J. Nucl. Sci. Technol.*, **40**, 559 (2003).
17) M. Ohta, S. Nakamura, H. Harada, T. Fujii, H. Yamana, "Measurement of effective capture cross section of americium-243 for thermal neutrons," *J. Nucl. Sci. Technol.*, **43**, 1441 (2006).
18) S. F. Mughabghab, M. Divadeenam, N. E. Holden, *Neutron Cross Section*, Academic Press, New York, vols. **1** and **2**, (1981).
19) S. F. Mughabghab, *Thermal Neutron Capture Cross Sections, Resonance Integrals, and g-factors*, INDC(NDS)-440, (2003).
20) C. H. Westcott, W. H. Walker, T. K. Alexander, *Proc. 2nd Int. Conf. Peaceful Use of Atomic Energy, Geneva*, United Nations, New York, **16**, 70 (1958).
21) A. Koning, R. Forrest, M. Kellett, R. Mills, H. Henrikson, Y. Rugama (Eds.), *The JEFF-3.1 Nuclear Data Library*, JEFF Report 21 (2006).
22) M. B. Chadwick, P. Oblozinsky, M. Herman, N. M. Greene, R. D. McKnight, D. L. Smith, P. G. Young, R. E. MacFarlane, G. M. Hale, S. C. Frankle, A. C. Kahler, T. Kawano, R. C. Little, D. G. Madland, P. Moller, R. D. Mosteller, P. R. Page, P. Talou, H. Trellue, M. C. White, W. B. Wilson, R. Arcilla, C. L. Dunford, S. F. Mughabghab, B. Pritychenko, D. Rochman, A. A. Sonzogni, C. R. Lubitz, T. H. Trumbull, J. P. Weinman, D. A. Brown, D. E. Cullen, D. P. Heinrichs, D. P. McNabb, H. Derrien, M. E. Dunn, N. M. Larson, L. C. Leal, A. D. Carlson, R. C. Block, J. B. Briggs, E. T. Cheng, H. C. Huria, M. L. Zerkle, K. S. Kozier, A. Courcelle, V. Pronyaev, S. C. van der Marck, "ENDF/B-VII.0: Next generation evaluated nuclear data library for nuclear science and technology," *Nucl. Data Sheets*, **102**, 2931 (2006).